Section: Radiology

Original Research Article

DYNAMIC MAGNETIC RESONANCE IMAGING IN PITUITARY ADENOMA IN PATIENTS WITH ELEVATED SERUM PROLACTIN LEVEL

Sana Sateesh[1], Geetanjali[2], Nishant Jajee[3]

[1]Consultant Radiologist, Aster RV Hospital, Bangalore, India.
[2]Consultant Radiologist, Aster CMI Hospital, Bangalore, India.
[3]D'Ortho, DNB Ortho Consultant Orthopaedician, United Hospitals Gulbarga, India.

Received : 10/09/2023
Received in revised form : 10/10/2023
Accepted : 22/10/2023

Keywords:
Dynamic MRI of the pituitary gland proves to be a valuable tool for confirming the diagnosis of pituitary adenomas, particularly in patients with elevated serum prolactin levels.

Corresponding Author:
Dr. Radha Bawage,
Email: radharameshbawage@gmail.com

DOI: 10.47009/jamp.2023.5.5.252

Source of Support: Nil,
Conflict of Interest: None declared

Int J Acad Med Pharm
2023; 5 (5); 1277-1284

Abstract

Background: Objectives: This study aims to assess the diagnostic efficacy of dynamic MRI in detecting pituitary adenomas, particularly in patients exhibiting elevated serum prolactin levels. **Materials and Methods:** A cross-sectional investigation was conducted in the Department of Radiodiagnosis and Imaging at VIMS & RC, Bengaluru. Patients with elevated serum prolactin levels were subjected to a dynamic MRI of the pituitary gland. The sample size was determined based on case availability over an 18-month period, resulting in a cohort of 37 patients. **Results:** The majority of subjects fell within the 21–40 years age bracket and were female, with infertility being the predominant presenting symptom. Among the 37 patients who underwent MRI, 42.3% exhibited positive findings on T1, with 92.3% of lesions appearing isointense. On T2, 19.2% displayed positive findings, while 80.8% were negative for lesions. Approximately 53.8% demonstrated isointensity, and 42.3% exhibited mixed intensities. Notably, 24.3% were diagnosed with microadenoma, and 45.9% with macroadenoma. The mean Prolactin levels were 149.45 ± 109.66 ng/ml, with those having microadenoma at 160.00 ± 127.62 ng/ml and macroadenoma at 422.65 ± 499.76 ng/ml. The posterior pituitary was discernible as separate from the nodule in 41.2% of macroadenoma cases. For microadenoma cases, 100% were confined within the sella, with 11.8% presenting cystic and hemorrhagic areas, 5.9% indenting the optic chiasma, and 82.4% exhibiting sella widening. In macroadenoma cases, 88.2% displayed isointensity. Among those diagnosed with microadenoma, 88.9% of lesions were isointense, and 11.1% were hyperintense. **Conclusion:** Dynamic MRI of the pituitary gland proves to be a valuable tool for confirming the diagnosis of pituitary adenomas, particularly in patients with elevated serum prolactin levels.

INTRODUCTION

The adult hypophysis typically measures < 1 cm in its greatest dimension, weighs <1 gram. The anterior, intermediate, and posterior lobes of the pituitary gland act as three separate endocrine organs, each characterized by distinct cell populations, secretory products, and regulatory mechanisms.

Three key imaging sequences are typically used in pituitary evaluations, often sufficient for diagnosis, especially in detecting microprolactinomas. The first step involves sagittal T1-weighted sequence, crucial for anatomical orientation. This sequence is vital for assessing lesions with suprasellar extension.

For suspected intrasellar lesions, confirmation can be achieved through coronal T1-weighted imaging after gadolinium injection (CE T1WI). Low contrast dose is recommended to prevent obscuring small intraglandular lesions. Delayed imaging is useful, especially for detecting very small microadenomas in conditions like Cushing's disease.

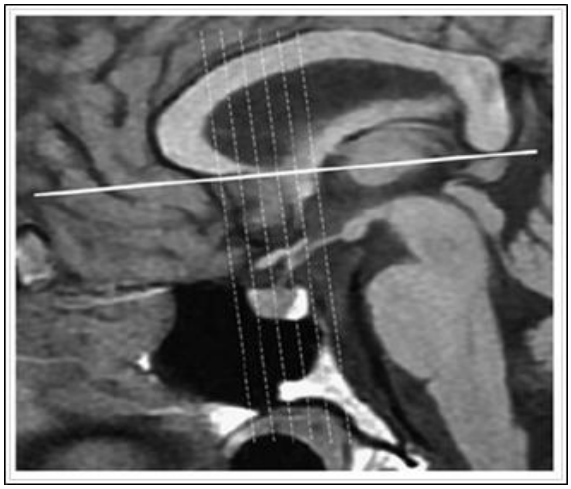

Figure 3: Sagittal T1WI

ISSN (O): 2687-5365; ISSN (P): 2753-6556

Axial T2 with fat saturation is highly valuable in confirming intrasellar Rathke cleft cysts, even when associated with pituitary microadenoma. 3D T1 gradient-echo sequence with very thin sections can reveal tiny ACTH-secreting pituitary microadenomas. Additionally, 3D TOF MRA is beneficial in assessing lesions in the cavernous sinus.[4]

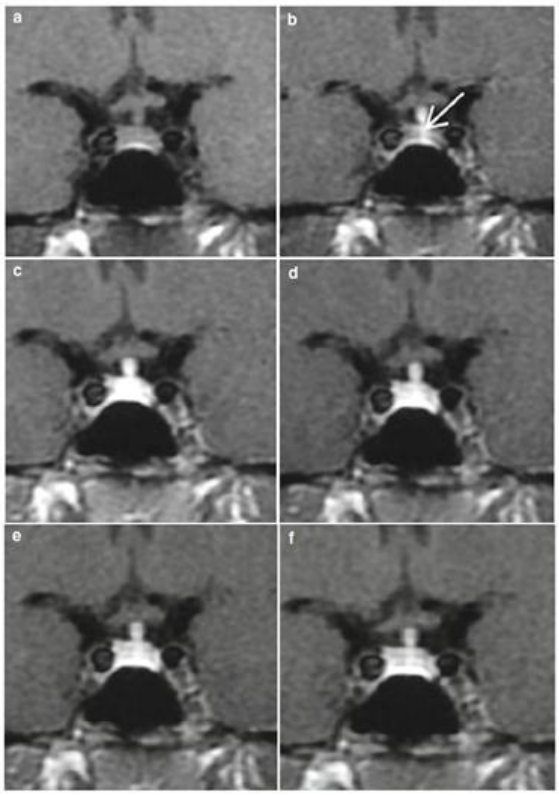

Figure 4: Dynamic MRI of normal pituitary gland. (a) Before contrast injection. (b) About 30sec later, opacification of the pituitary stalk and secondary capillary bed (arrow). (c) At 60sec, the enhancement of the pituitary gland is intense and homogeneous. (d–f) Slow decrease of enhancement intensity

Diffusion, perfusion imaging, and MR spectroscopy are helpful in distinguishing various pituitary and hypothalamic lesions. Diffusion imaging is crucial for early detection of conditions like pituitary infarction and differentiating abscesses from hemorrhages. MR spectroscopy offer distinct metabolic profiles in different lesions like gliomas, craniopharyngiomas, germinomas, hamartomas, adenomas, aiding in their differentiation.

MRI anatomy of the pituitary gland

Anterior Lobe of the Pituitary Gland

Normally, it shows a uniform signal like the temporal lobe's white matter on T1WI. The gland's size and shape vary with age and gender, being rounder and larger in infants under one month (63% convex), compared to older children (4% convex).

Under typical conditions, the upper part of the pituitary stalk is thicker than the lower, but a tube-like appearance doesn't definitively indicate pituitary microadenoma. The posterior lobe of the pituitary gland exhibits a bright signal on T1-weighted images, indicating normal vasopressin storage; it's absent in central diabetes insipidus.

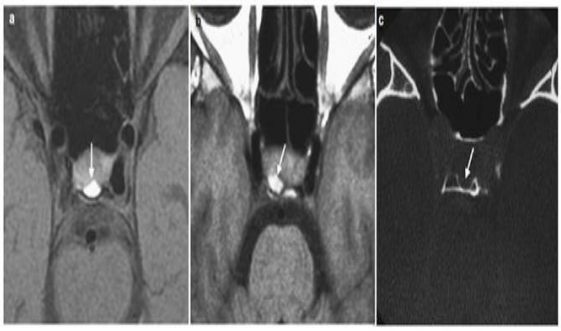

Figure 5: Normal posterior lobe of the pituitary gland. (a)Axial Fat-Sat T1WI at 3.0 T. Suppression of the fat signal of the dorsum sellae allows good delineation of the hyperintense posterior lobe (arrow). (b) Axial T1WI at1.5 T. Lateralized posterior lobe. (c) Axial CT scan, bone window demonstrating the imprint of the posterior lobe in the dorsum sellae (fossula hypophyseos) (arrow)

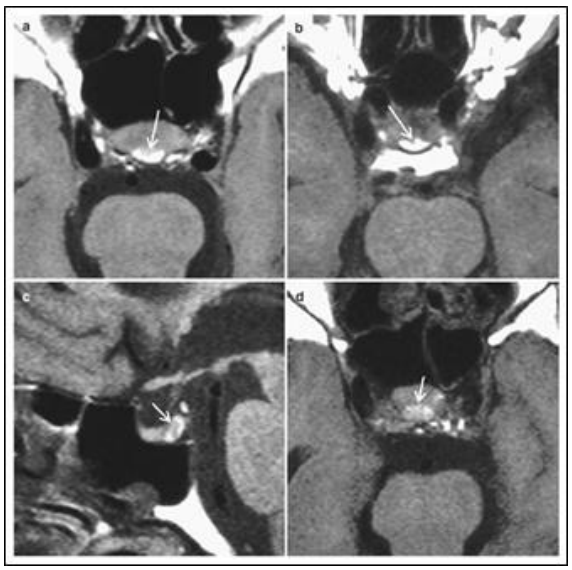

Figure 6: Variants of posterior lobe. (a,b) Axial T1WIs in two elderly subjects. Heterogeneous appearance and irregularities of the anterior aspect of the posterior lobe (arrow). (c,d) Axial T1WIs in a 78-year-old woman. The posterior lobe is faintly hyperintense.

Due to persistently raised plasmatic osmolality lesser T1 hyperintensity can be observed during pregnancy, patients undergoing hemodialysis or with uncontrolled diabetes mellitus, severe anorexia nervosa, and in a stressed condition.[17]

Cavernous Sinus: Before gadolinium injection, internal carotid arteries show low signal due to rapid flow, indicating a "flow void." The absence of the carotid sulcus vein suggests potential cavernous sinus invasion by a pituitary adenoma.

ISSN (O): 2687-5365; ISSN (P): 2753-6556

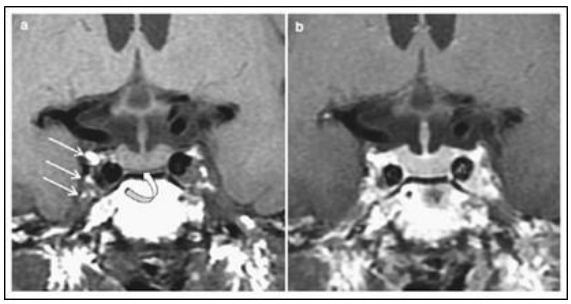

Figure 7: Normal cavernous sinus. (a) Coronal T1WI and (b) CE T1WI. The low- flow veins appear hyperintense on T1WI and CE T1WI (arrows). A thin inferior intercavernous sinus is demonstrated in contact with the sellar floor (curved arrow)

High-resolution spin-echo T1WI and fast spin-echo T2WI allow the visualization of the internal architecture of the Meckel cave. The tracts of nervous fibers that constitute the trigeminal nerve in the Meckel cave can be identified within the CSF, especially on T2WI.[4]

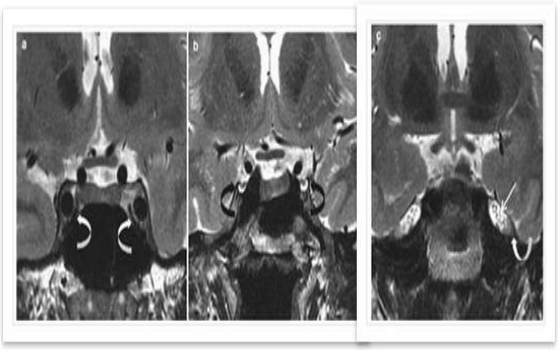

Figure 8: Normal cavernous sinus. Coronal T2WIs. (a) Bilateral veins of the carotid sulcus located between the sphenoid sinus lateral wall and the intracavernous internal carotid artery (curved arrows). (b) The oculomotor nerves, well delineated by their CSF- filled sheaths, are identified at the upper compartment of the cavernous sinus (black curved arrows). (c) Posterior cut through the Meckel cave. The tracts of nervous fibers constituting the trigeminal nerve (arrow) are seen in the CSF of both the Meckel cave and the trigeminal ganglia (curved arrow)

Clinically relevant pituitary adenomas is 1 per 1000–1300 of the general population. Mostly, are benign and usually occur sporadically. By patient history, physical examination, various tests, including blood and urine tests to check hormone levels, brain imaging (CT or MRI) to locate and measure the tumor, vision testing to assess any impact on sight.[10] Hyperprolactinemia results from elevated levels of prolactin in the blood, often due to a pituitary gland tumor called prolactinoma. This condition can cause infertility, decreased sex drive, bone loss, and various symptoms in both men and women. Diagnosis involves blood tests and, if a prolactinoma is suspected, an MRI of the brain and pituitary.[11]

Radiographic features of pituitary adenoma and microadenoma

Pituitary microadenomas are a minority of all pituitary adenomas but can pose imaging and management challenges on account of their size and clinical presentations. By definition, a microadenoma is <10 mm and if tumor is >10 mm in size, it is then considered pituitary macroadenoma.[14]

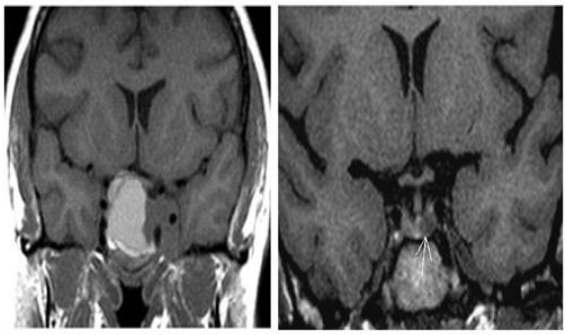

Figure 9: A coronal unenhanced T1 weighted image shows a small left sided microadenoma (arrow) as an area of lower signal than the rest of the anterior pituitary tissue.

Prolactinomas are the most common microadenomas and usually are accompanied by amenorrhea and galactorrhea in women. They are commonly hypointense to pituitary gland on T1 images, occasionally isointense. On T2 images appearance is variable.

At some point after the administration of contrast material, the adenoma ―wash-in will equal the pituitary gland wash-out, making the lesion inconspicuous. Lesions that are isointense on initial images may be clearly visualized only after contrast material administration. Secondary signs of microadenomas include lateral deviation of the infundibulum and focal upward convexity of the pituitary gland.[15]

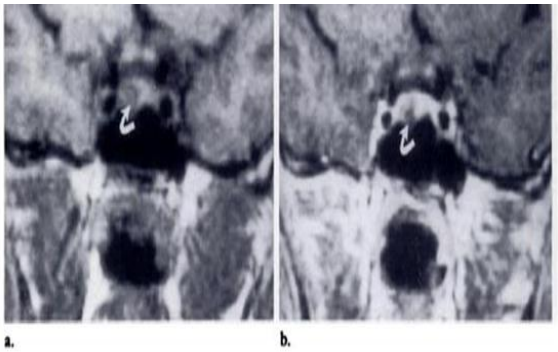

Figure 10: Microadenoma. (a) Coronal T1W MR image shows 4-mm hypointense lesion (arrow) located within pituitary gland, to right of the midline. (b) On enhanced coronal T1W MR image, the hypointense lesion (arrow) becomes more apparent against enhanced gland immediately after administration of contrast material

Pituitary macroadenomas

Pituitary macroadenomas can extend superiorly into the suprasellar cistern and impinge on the optic nerves and/or optic chiasm to produce visual field abnormalities (typically a bitemporal hemianopia).

ISSN (O): 2687-5365; ISSN (P): 2753-6556

Pituitary macroadenomas with a large suprasellar component characteristically show the appearance of ―waisting as they pass through the diaphragma sellae.

Lateral growth of a macroadenoma is first seen to cause deformity of the cavernous sinus; however, adenomas can invade into the cavernous sinus. If MR imaging demonstrates adenoma tissue extending most lateral margin of the cavernous segment, then very likely that there is tumor within the cavernous sinus. Adenomas can also extend inferiorly into the sphenoid producing remodelling of the bone.

Table 3: Summary of Pituitary Gland Disorders with MRI Characteristics

Condition	Description	MRI Characteristics
Meningioma	Common extra-axial tumor arising from the dura mater. Isointense to gray matter on T1 and T2-weighted MRI, homogeneous moderate to avid enhancement after gadolinium contrast.	T1: Isointense, T2: Isointense, Homogeneous Enhancement
Craniopharyngioma	Nonglial tumors with two subtypes: adamantinomatous and papillary. Variable MRI characteristics based on subtype.	Characteristics vary depending on the subtype.
Chordoma	Locally aggressive tumors derived from notochord remnants. Bright on T2-weighted MRI. Different subtypes.	T2: Bright
Chondrosarcoma	Well-circumscribed, hyperintense on T2-weighted sequences, may lead to ophthalmoplegia due to lateral location.	T2: Hyperintense, May Cause Ophthalmoplegia
Schwannoma	Arise from cranial nerves. Isointense to gray matter on T1, heterogeneously hyperintense on T2-weighted MRI.	T1: Isointense, T2: Heterogeneously Hyperintense
Optic Pathway Glioma	More common in children. Involves optic nerves, chiasm, and tracts. MRI characteristics include enlargement and variable enhancement.	Enlargement, Variable Signal Intensities, Enhancement
Germ Cell Tumor	Common subtype of intracranial germ cell tumors. Restricted diffusion on MRI, similar imaging for different histologic subtypes.	Restricted Diffusion
Plasmacytoma	Plasma cell neoplasms, may exhibit intrinsic T1 hyperintensity, relatively isointense to gray matter on T2.	T1: Hyperintense, T2: Isointense
Metastases	Occur in some cancer patients. Hypointense regions on T1-weighted sequences, evaluate for potential CSF seeding.	T1: Hypointense, Evaluate for CSF Seeding
Rathke Cleft Cyst	Benign epithelial cysts. May be hyperintense on T2-weighted MRI, with a T1-hyperintense, T2-hypointense intracystic nodule.	T2: Hyperintense, T1: Hyperintense Nodule
Dermoid and Epidermoid Tumor	Nonneoplastic lesions with distinct origins. May appear hyperintense on diffusion-weighted sequences, dermoids follow fat characteristics on CT and MRI.	Hyperintense on DWI, Fat Characteristics on CT and MRI
Arachnoid Cyst	Benign, nonneoplastic cysts filled with CSF. Follow CSF signal intensity on MRI, suppress on FLAIR.	Follow CSF Signal Intensity, Suppress on FLAIR
Hypothalamic Hamartoma	Benign lesions arising from neuronal and glial tissues. May cause gelastic seizures. MRI does not strictly follow gray matter signal intensity.	Does Not Follow Strict Gray Matter Signal Intensity
Giant Aneurysm	Can lead to osseous erosion of the skull base. Heterogeneous signal intensities, incomplete enhancement, pulsation artifact.	Heterogeneous Signal, Incomplete Enhancement, Pulsation Artifact
Sarcoidosis	Can involve various parts of the brain, meninges, and cranial nerves. Lesions may exhibit leptomeningeal or pachymeningeal thickening and enhancement.	Leptomeningeal or Pachymeningeal Thickening and Enhancement
Lymphocytic Hypophysitis	Infiltrative autoimmune/inflammatory disorder. May lead to thickening and avid enhancement of the pituitary gland. T2-hypointense area in the parasellar region.	Thickening and Avid Enhancement of Pituitary Gland, T2-Hypointense Area

Dynamic MR imaging has emerged as a promising tool in the evaluation of pituitary adenomas, particularly in accurate delineation of those microadenomas with no contour abnormality, and in differentiating residual/recurrent adenoma from surrounding post-operative tissue. Dynamic MR imaging is useful in the evaluation of pituitary microadenomas and macroadenomas.

Dynamic MRI technique captures a temporal phase in which there is a high level of contrast between the tumor and the normal pituitary gland.

MATERIALS AND METHODS

A cross-sectional study was undertaken in the Department of Radio Diagnosis and Imaging in VIMS & RC, Bengaluru. Patients with elevated levels of serum prolactin were subjected to Dynamic Magnetic resonance imaging of the pituitary gland. Ethical clearance was obtained before the study was started. Informed, bilingual, and written consent was obtained before including them in the study. The calculated sample size was 34 who were newly diagnosed, depending upon the availability of the cases during the time period, the sample size was increased to 37. The inclusion and exclusion criteria were as follows:

Inclusion Criteria

All patients with elevated serum prolactin levels will be subjected to Dynamic Magnetic Resonance Imaging.

Patients with serum prolactin >29ng/ml in females and > 18ng/ml in males.

Exclusion Criteria

Patients with normal serum prolactin levels.

Patients having an allergic reaction to contrast.

Patients who were claustrophobic had a pacemaker or prewire grant.

ISSN (O): 2687-5365; ISSN (P): 2753-6556

Metallic foreign body in the orbi, aneurysm clip, or patients with no prolactin levels.

Other causes of hyperprolactinemia such as tuberculosis, chest wall lesions, sarcoidosis, and metabolic disturbances.

All patients referred to the Department of Radio diagnosed with elevated prolactin levels in a period of 18 months were subjected to a Dynamic MRI of the rain for the pituitary.

MRI examinations were performed with PHILPS ACHIEVA (1.5 Tesla MRI scanner). A multichannel phased array head coil was used for signal excitation. MRI protocols included the following sequences: T1-weighted spin-echo, with 3mm contiguous coronal slices; T2-weighted spin-echo, with 3mm contiguous coronal slices; and a sagittal T1 acquisition. Dynamic contrast study will be done with T1 Fast spin echo technique Gadodiamide (0.1mmol/kg) administered over 60 seconds by hand injection. Dynamic coronal images were obtained simultaneously from three different portions of the gland at an interval of 20-30 seconds between the images. The dynamic scan duration will be 120-140 seconds.

Statistical Analysis

Data was entered into a Microsoft Excel data sheet and was analyzed using SPSS 22 version software. Categorical data was represented in the form of Frequencies and proportions. The chi-square test was used as a test of significance for qualitative data. Kruskal Wallis test was the test of significance to identify the mean difference between more than two groups for qualitative data. Graphical representation of data: MS Excel and MS word was used to obtain various types of graphs such as a badiagram and m, anaie diagram-value (Probability that the result is true) of <0.05 was considered as statistically significant after assuming all the rules of statistical tests. Statistical software: MS Excel, SPSS version 22 (IBM SPSS Statistics, Somers NY, USA) was used to analyze data.

DISCUSSION

In the human body, the pituitary gland is considered ―the master gland. The literature available shows that about 15 – 20% of the intracranial neoplasms - pituitary adenomas (21). The imaging of the pituitary gland in patients with raised prolactin may help in detecting and confirming the diagnosis.

The Dynamic MRI has proven to be the best imaging tool for evaluation of the pituitary adenomas, particularly in accurate delineation of those microadenomas with no contour abnormality, and in differentiating residual/ recurrent adenoma from surrounding post-operative tissue.

In the study 13.5% were in the age group <20 years, 27% were in the age group 21 to 30 years, 27% were in the age group 31 to 40 years, 16.2% were in the age group 41 to 50 years and 16.2% were in the age group >50 years (Table 4). A similar study by Pereira et al had shown that most of the cases belonged to 31 – 40 years and 41 – 50 years age group.

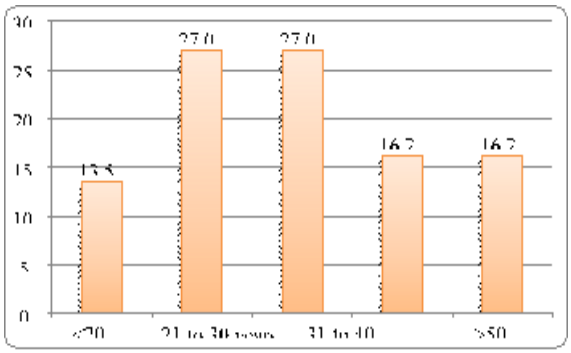

Graph 1: Bar diagram showing Age distribution of subjects in the study

The majority of the patients (45%) in this study had infertility as the main presenting symptom of Pituitary adenoma. This was followed by unexpected lactation (24.3%), Secondary infertility hypermenorrhea (10.8%), hypermenorrhea (8.1%), secondary infertility (8.1%), and headache in 2.7% of the cases (Table 6). In a study of pituitary tumors by Periera et al, about 30% of the cases presented with headache, 25% with visual disturbances, 33% with acromegaly and 1.6% with amenorrhea, 2% with menstrual irregularity, 2% with galactorrhoea and 6% with menstrual irregularity and galactorrhea

In this study, T1 weighted images of MRI has shown that, 42.3% were positive for lesion and 57.7% were negative for lesion. About 92.3% of lesions were isointense and 7.7% were mixed (iso intense and hyper intense) (Table 7). A study by Azeemuddin et al had shown that, the MRI revealed the lesions in 55.7% of the study subjects.

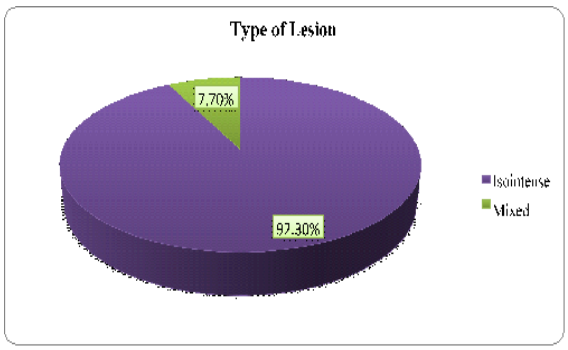

Graph 3: Pie diagram showing T1 Lesion detection and characteristics

T2 weighted images of MRI had shown that, 19.2% were positive for lesion and 80.8% were negative for lesion as 53.8% were isointense, 42.3% were mixed intense and 3.9% were hyperintense lesions (Table 8).

ISSN (O): 2687-5365; ISSN (P): 2753-6556

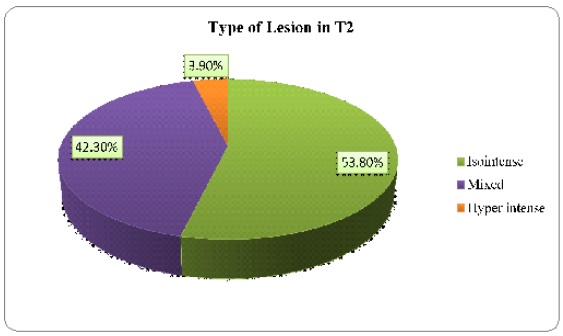

Graph 4: Pie diagram showing T2 Lesion detection and characteristics

In the study 29.7% were normal, 24.3% were diagnosed to have microadenoma and 45.9% had macroadenoma (Graph 5). In a study by Periera et al, the sellar macroadenomas were seen in 20.7% of the cases, and sellar with suprasellar extension was seen in 43.5% of the cases, sellar with sphenoid sinus invasion were occurred in 7.5% of the cases.

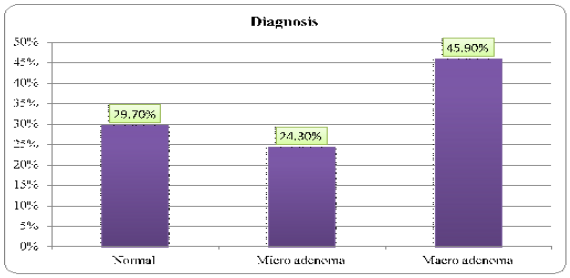

Graph 5: Bar diagram showing Diagnosis in the study subjects

In the study among those who were normal, the mean Prolactin levels was 149.45 ± 109.66 ng/ml, those with microadenoma had a mean value of 160.00 ± 127.62 ng/ml and those with macro adenoma had 422.65 ± 499.76 ng/ml. Rand et al had noticed that, the the mean prolactin level was 155.72 ng/ml in patients with macroadenomas in comparison with 110.14 ng/ml in patients with microadenomas.

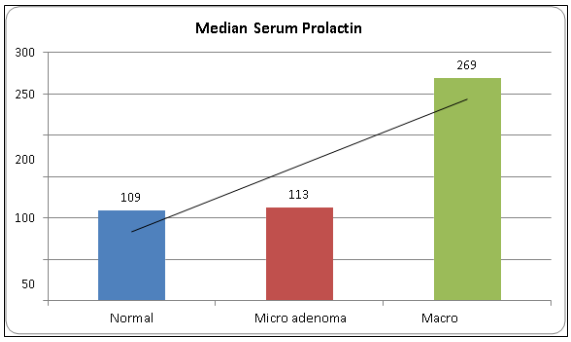

Graph 6: Bar diagram showing Correlation of Serum Prolactin levels with respect to diagnosis in the study subjects

This study had shown that, all the microadenoma had nodule size of less than 10 mm and all those with macro adenoma had nodule size > 10 mm (Table 12). In a study by Periera et al, the pituitary macroadenomas size ranged from 1 – 3 cm in 41.5% of the cases and 3 – 5 cm in 58.5% of the cases.

Table 6: Association between Diagnosis and Nodule size

		Nodule size					
		No Nodule		<10		>10	
		Frequency	Percent	Frequency	Percent	Frequency	Percent
Diagnosis	Normal	11	100.0%	0	0.0%	0	0.0%
	Micro adenoma	0	0.0%	9	100.0%	0	0.0%
	Macro adenoma	0	0.0%	0	0.0%	17	100.0%

$\chi 2 = 74$, df = 4, p <0.001*(significant)

In the study among those with microadenoma, 100% posterior pituitary was seen separately from nodule and those with macroadenoma, in 41.2% posterior pituitary was seen separately from nodule (Table 13). There was significant association between diagnosis of adenomas and posterior pituitary seen separately from nodule. No studies compared these results.

Table 7: Association between Diagnosis and Posterior pituitary seen separately from nodule

		Posterior pituitary seen separately from nodule					
		No lesion		No		Yes	
		Frequency	Percent	Frequency	Percent	Frequency	Percent
Diagnosis	Normal	11	100.0%	0	0.0%	0	0.0%
	Micro adenoma	0	0.0%	0	0.0%	9	100.0%
	Macro adenoma	3	17.6%	7	41.2%	7	41.2%

$\chi 2 = 36.18$, df = 4, p <0.001*(Significant)

In those with micro adenoma, 100% were confined within sella, those with 11.8% were cystic and hemorrhagic areas, 5.9% were indenting optic chiasma and 82.4% had widening of sella (Table 14). There was significant association between diagnosis and Primary sign. A tumour of more than 10 mm pituitary adenoma may be situated near to optic chiasma if the sella turcica is small or flat. The modifications in the sellar floor are more difficult to distinguish in MR imaging than on a CT scan.

ISSN (O): 2687-5365; ISSN (P): 2753-6556

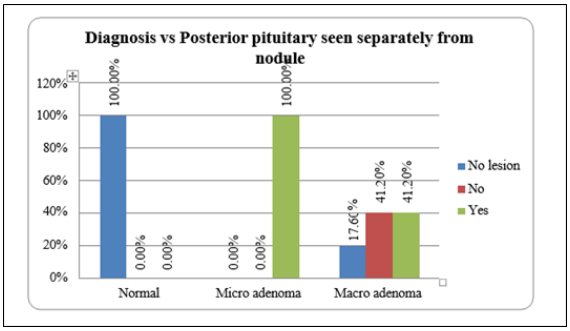

Graph 7: Association between Diagnosis and Posterior pituitary seen separately from the nodule

In the study among those with microadenoma, 100% had Isointense lesion and in those with macro adenoma, 88.2% had Isointense lesion and 11.8% had Mixed lesion (Table 16). In a study by Periera et al, the homogenous signal intensity was present in 60.4% of the cases and 39.6% showed heterogenous signal intensity. The macroadenoma appeared hypointense on T1WI.

In the study among those who were diagnosed to have microadenoma, 88.9% of lesions were Isointense, 11.1% were hyper intense. Those with macroadenoma, 35.3% had iso intense and 64.7% were mixed lesions. There was significant association between T2 MRI findings and diagnosis (Table 17). In a study by Periera et al, the macroadenomas appeared hyperintense on T2 WI.

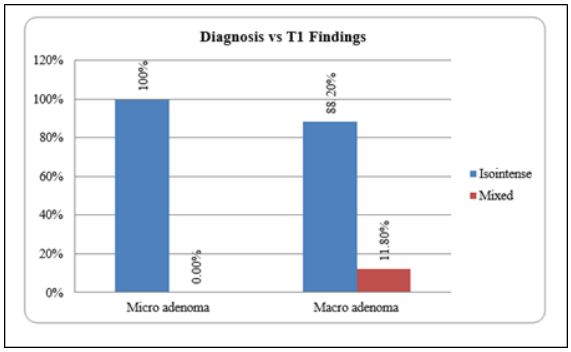

Graph 8: Bar diagram showing Association between Diagnosis and T1 Findings

In the study among those with microadenoma, 100% had late enhancement and those with macro adenoma, 100% had early enhanc ement (Table 15). There was significant association between diagnosis and dynamic enhancement. Out of 37 patients, 26 patients showed characteristics of pituitary adenoma. No studies were available to compare these results.

Table 8: Association between Diagnosis and Dynamic Enhancement

		Dynamic Enhancement			
		Early		Late	
		Frequency	Percent	Frequency	Percent
Diagnosis	Micro adenoma	0	0.0%	9	100.0%
	Macro adenoma	17	100.0%	0	0.0%

In the study 65.4% had early enhancement and 34.6% had late enhancement (Table 9). The studies were not available to compare these findings. The macroadenomas with early enhancement pattern are significantly more fibrous and receive direct blood supply from the superior hypophyseal artery. After bolus injection of the contrast, the enhancement first occurs in the pituitary stalk, then the pituitary tuft and then there in centrifugal enhancement of the anterior lobe. Within 30-60seconds, entire lobe shows homogenous enhancement. Hence, microadenomas appear as relatively non-enhancing lesions within an intensely enhancing pituitary gland. Furthermore, microadenomas do not receive direct blood supply from the superior hypophyseal artery. Perforators from the superior hypophyseal artery supply the microadenomas, hence it enhances late.

Limitations

However, this study is not without limitations. It was a cross-sectional study that lacked surgical and histopathological diagnosis to prove the presence of adenomas. In this study, there was a significant correlation between elevated serum prolactin levels and pituitary adenomas. Out of 37 patients, 17 patients had macroadenoma and 9 patients had microadenoma. However, 11 patients who had elevated serum prolactin had no positive findings on Dynamic MRI. This disparity is due to a limited caseload. However, this study was able to bring out many facts about the diagnosis of pituitary prolactin-secreting adenomas. More research is needed regarding the study of dynamic MRI in pituitary tumor imaging.

CONCLUSION

Dynamic contrast magnetic resonance imaging helps in detecting the presence of pituitary adenomas in patients with elevated serum prolactin levels and MRI with DCE should be included as a primary imaging modality in all cases of elevated prolactin levels of pituitary adenomas secreting prolactin. The study showed that, pituitary adenomas commonly occur in young women. Infertility was the main presenting symptom. The pituitary adenomas presented as isointense lesions on T1 and T2 weighted imaging on MRI.

REFERENCES

1. Bonneville, Jean-François, et al. Advances in understanding pituitary tumors. 2016;1:1-11.
2. Evans VR, Manning AB, Bernard LH, Chronwall et.al localized in the human pituitary but are not restricted to the zona intermedia. Endocrinology. 1994 Jan. 134(1):97-106.

ISSN (O): 2687-5365; ISSN (P): 2753-6556

3. Davis SW, Ellsworth BS, Millan MIP, et al. Pituitary Gland Development and Disease: From Stem Cell to Hormone Production. Curr Top Dev Biol. 2013;106:1–47.
4. Indrajit IK, Chidambaranathan N, Sundar K, et al. Value of dynamic MRI imaging in pituitary adenomas. Neuroradiology. 2001;11(4):185-190.
5. Beckers A, Rostomyan L, and Daly AF. Overview of genetic testing in patients with pituitary adenomas. Annales d'Endocrinologie. 2012;73:62–64.
6. Jiang X and Zhang X. The Molecular Pathogenesis of Pituitary Adenomas: An Update. Endocrinol Metab. 2013;28:245–254.
7. Molitch ME. Diagnosis and Treatment of Pituitary Adenomas: A Review. JAMA. 2017;317(5):516-524.
8. Harefuah. Radiosurgery for pituitary adenomas. 2017;156(1):45-50.
9. F.A.Daly, C.M.Burlacu, et al. The epidemiology and management of pituitary incidentalomas. 2007;68:195-198.
10. I.S.Tamer, O.Ronald, et al. MR Imaging: Brief overview and Emerging applications. 2007;27:1213-1226.
11. P.A.Robert. Fundamental physics of MR Imaging. 2005;25:1087-1099.
12. N.Denis, B.L.Robert and P.G.Hollis. What are the advantages and disadvantages of Imaging modalities to diagnose wear-related corrosion problems. 2014;472:3665-3673.
13. Jobnsen DE, Woodruff WW, Allen IS, et al. MR Imaging of the Sellar and Juxtasellar Regions. Radiographics. 1991;11:727–758.
14. Go JL and Rajamohan AG. Imaging of the Sella and Parasellar Region. Radiol Clin N Am. 20147;55:83–101.
15. Indrajit IK, Chidambaranathan N, Sundar K, et al. Value of dynamic MRI imaging in pituitary adenomas. Indian J Radiol Imaging. 2001;11:185–190.
16. Moisi M, Cruz AS, Benkers T. Treatment of Aggressive Prolactin-Secreting Pituitary Adenomas with Adjuvant Temozolomide Chemotherapy: A Review. Cureus 2016;8(6):e658.
17. Kawaguchi T, Ogawa Y and Tominaga T. Diagnostic pitfalls of hyperprolactinemia: the importance of sequential pituitary imaging. BMC Research Notes. 2014;7:555.
18. . Azeemuddin M, Naqi R and Wasay M. A descriptive study to find possible correlation between MRI findings of pituitary gland and serum prolactin level. Journal of Pakistan Medical Association. 2013;63(6):739–742.
19. Ezzat S, Asa SL, Couldwell WT, et al. The Prevalence of Pituitary Adenomas. CANCER. 2004;101(3):613–619.
20. Caporalini C, Buccoliero AM, Pansini L, et al. Pituitary adenoma with adipose tissue: A new metaplastic variant. Neuropathology. 2017;37(4):329–334.
21. Molitch ME. Diagnosis and Treatment of Pituitary Adenomas: A Review. JAMA. 2017;317(5):516–524.
22. Park S, Kang S, Lee HW, et al. Central Prolactin Modulates Insulin Sensitivity and Insulin Secretion in Diabetic Rats. Neuroendocrinology. 2012;95:332–343
23. Lundberg PO, Osterman PO and Wide AL. Serum prolactin in patients with hypothalamus and pituitary disorders. J Neurosurg. 1981;55:194–199.
24. Chaudhary V and Bano S. Imaging of the pituitary: Recent advances. Indian J Endocrinol Metab. 2011;15(3):S216–S223.
25. Indrajit IK, Chidambaranathan N, Sundar K, et al. Value of dynamic MRI imaging in pituitary adenomas. Neuroradiology. 2001;11(4):185-190.
26. Z. Gabriel, C John, et al. Pituitary adenoma. British journal of medicine. 2018; Accessed on September 6, 2018.
27. Bonneville JF, Bonnevillae F, Cattin F, Magnetic resonance imaging of pituitary adenomas, Eur Radiol : 2005: 15: 543–548.
28. Theodros D, Patel M, Ruzevick J, et al. Pituitary adenomas: historical perspective, surgical management and future directions. CNS Oncol. 2015;4(6):411–429.

ISSN (O): 2687-5365; ISSN (P): 2753-6556